Available online at www.sciencedirect.com
ScienceDirect
Journal of Sound and Vibration 318 (2008) 820–829
JOURNAL OF SOUND AND VIBRATION
www.elsevier.com/locate/jsvi

Identification of damage in beam structures using flexural wave propagation characteristics

Junhong Park*

School of Mechanical Engineering, Hanyang University, 17 Haengdang-dong, Seongdong-gu, Seoul 133-791, South Korea

Received 17 August 2007; received in revised form 25 February 2008; accepted 4 May 2008
Handling Editor L.G. Tham
Available online 24 June 2008

Abstract

An experimental method of detecting damage using the flexural wave propagation characteristics is proposed. To monitor change in structural properties due to damage, the frequency-dependent variation of the wavenumber, wave speed, and the dynamic properties were measured in the frequency ranges of flexural vibration. The measured frequency-dependent variation was compared to those measured when undamaged. The beam transfer function method was used to obtain the dynamic properties. The location and magnitude of damage were identified using the property that it has significant impact on the system potential energy. When the wave propagates through a medium, the total system energy remains mostly unchanged, but its form changes between potential and kinetic energy. The wave propagation characteristics are affected most when damage occurs at locations where the wave energy is in the form of the potential energy. The validity of the proposed method was confirmed by experimentation. The various locations of damage imposed on the beam structures with different magnitudes were identified accurately.

1. Introduction

As structures become bigger, wider and heavier, and as they are used for longer periods of time, the need for practical methods of monitoring structural integrity has increased. Widely used methods of non-destructive structural integrity evaluation include visual inspection, X-ray and ultrasound. However, these methods require too long time for inspecting every part of structures and are not practical for real-time health monitoring. Also, additional hardware is required for excitation of structures and collection of vibration data. Consequently, low-frequency vibration methods to determine the size and location of damage in structures have attracted research interest because of their efficiency in structural health monitoring [1].

The natural frequencies of the given systems have most often been used by researchers [2–4]. Crack location has been predicted accurately by minimizing the difference between measured and predicted values through the analysis of the effects of crack locations on several natural frequencies. This method requires a small number of vibration measurements. However, it is difficult to identify effects from the surrounding environment. Also, the measured natural frequency does not show significant change for damage induced at a nodal point [5]. A more

*Tel.: +82 2 2220 0424.
E-mail address: parkj@hanyang.ac.kr

0022-460X/$ - see front matter © 2008 Elsevier Ltd. All rights reserved.
doi:10.1016/j.jsv.2008.05.008

sensitive method was proposed based on the mode shape of the structure [1,5–7]. In this approach, many sensors are required to detect the mode shapes of the higher-order modes, which could cause practical problems in installation and maintenance. Adams and Nataraju [8] proposed a structural diagnostic method using nonlinear vibration characteristics resulting from structural defects. Since the vibration is analyzed based on modal properties, the method is applicable to arbitrary complex structures. For random vibrations, the variation of the kurtosis with crack depth was estimated and used in the damage detection [9]. Ma and Pines [10] proposed a damage identification method by using dereverberation of the measured transfer function. The dereverberated transfer function represents the direct path of energy transfer. It is not as frequency dependent as compared with the measured transfer function. Using the dereverberated transfer function, the occurrence of damage between sensors installed along the structure was estimated. Lamb waves have been widely used as methods of detecting structural defects [11–13]. The wavelength of the Lamb wave which propagates at much higher frequencies than the fundamental frequency of the system is small. Lamb wave diffraction can occur even from small defects in a structure. For structural diagnosis, a qualitative method based on impedance monitoring techniques was proposed [14–16]. The impedance monitoring method requires a small number of measurements at high frequencies for advantages related to high sensitivity to small defects.

In this study a new method based on the flexural wave propagation characteristics is proposed. As the flexural wave propagates, the total system energy remains mostly unchanged, but its form varies between strain (or potential) and kinetic energy. When damage occurred at locations where the wave energy is stored as the potential energy, there is a significant impact on the standing wave patterns. The beam transfer function method [16] was used to analyze the flexural wave propagations. Since the beam transfer function method is based on theoretical solutions of structural vibration, it required fewer (two or three) vibration measurements. The obtained frequency-dependent variation of the wave propagation characteristics are sensitive to measured transfer functions which represent the current structural integrity. The location and severity of damage was estimated using the measured dynamic properties. Since the result from the beam transfer function method is a continuous variation of the dynamic properties with frequency, effects of surrounding environment are minimized, and modal property measurements are not necessary.

2. Damage identification

2.1. Equivalent dynamic properties

When damage occurred in the cross-sectional area of structures, it results in a significant reduction in load-carrying capacity. Thus there is a reduction in the stored potential energy. When the effects of shear deformation and rotary inertia are negligible compared to those of bending deformation, the potential and kinetic energy of a vibrating beam is obtained respectively as

$$V = \int_0^L \frac{1}{2} D \left(\frac{\partial^2 w}{\partial x^2} \right)^2 \mathrm{d}x, \quad T = \int_0^L \frac{1}{2} M \left(\frac{\partial^2 w}{\partial t^2} \right)^2 \mathrm{d}x, \tag{1a,b}$$

where w is the flexural displacement, D is the bending stiffness, M is the mass per unit length and L is the length. The total potential energy stored in the system is determined by the standing wave pattern, Fig. 1. The standing wave pattern depends on the boundary conditions, and Fig. 1 shows potential and kinetic energy for the cantilever beam at different frequencies. When damage occurred at locations of large potential energy, the reduction of the potential energy is large. But the damage has negligible impact on the system kinetic energy. In this study, the equivalent dynamic properties obtained using the structural wavenumber is used to estimate this change, Fig. 2. The equation of motion for vibrating beams is obtained as

$$D \frac{\partial^4 w}{\partial x^4} + M \frac{\partial^2 w}{\partial t^2} = 0. \tag{2}$$

Assuming harmonic motion, i.e., $w(x,t) = \mathrm{Re}\{\hat{w}(x)\mathrm{e}^{\mathrm{i}\omega t}\}$, the separation of variables to solve Eq. (2) is performed. To model the dissipation of vibration energy within a structure, complex stiffness is used:

$$\hat{D}(\omega) = D(\omega)[1 + \mathrm{i}\eta_D(\omega)], \tag{3}$$

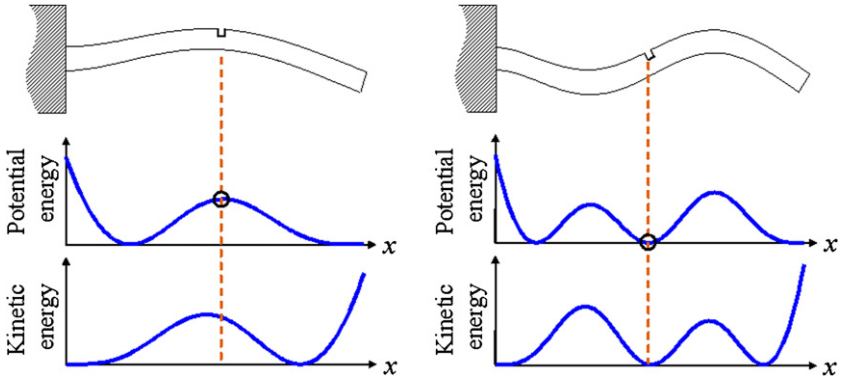

Fig. 1. Dependence of the potential and kinetic energy on the damage location and standing wave pattern.

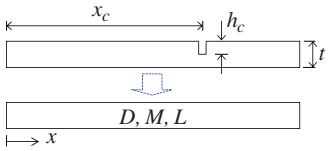

Fig. 2. Equivalent dynamic properties of a beam structure.

where η_D is the loss factor and $D(\omega)$ is the dynamic bending stiffness. For undamaged beam the bending stiffness is obtained as $E(\omega)t^3b/12$ where $E(\omega)$ is the elastic modulus and b is the width of the beam. For the damaged beam, the equivalent dynamic bending stiffness can be smaller or larger than those measured for undamaged structures. In most cases, it is expected that the dynamic bending stiffness decreases with an increasing magnitude of damage due to reduction in the system potential energy.

2.2. Sensitivity of dynamic bending stiffness on damage location

The wave propagation approach is used to obtain the sensitivity of the dynamic bending stiffness on the damage location. The satisfying beam function of Eq. (2) is

$$\hat{w}(x) = \hat{A}_1 \sin \hat{k}_b x + \hat{A}_2 \cos \hat{k}_b x + \hat{A}_3 e^{\hat{k}_b(x-L)} + \hat{A}_4 e^{-\hat{k}_b x}, \tag{4}$$

where $\hat{k}_b$ is the wavenumber related to the circular frequency through $\hat{k}_b = (\omega^2 M/\hat{D})^{1/4}$. $\hat{A}_1$ and $\hat{A}_2$ are the complex amplitudes of propagating waves. $\hat{A}_3$ and $\hat{A}_4$ are the magnitudes of exponentially decaying waves at $x = L$ and $x = 0$, respectively. When the cantilever beam was excited at its free end, the four boundary conditions are imposed as

$$\hat{w}(0) = 0, \quad \frac{\partial \hat{w}(0)}{\partial x} = 0, \quad \frac{\partial^2 \hat{w}(L)}{\partial^2 x} = 0, \quad \hat{D}\frac{\partial^3 \hat{w}(L)}{\partial^3 x} = F, \tag{5a–d}$$

where F is the force applied at $x = L$. The following matrix system of equations is obtained as

$$\begin{bmatrix} 0 & 1 & e^{-\hat{k}_b L} & 1 \\ 1 & 0 & e^{-\hat{k}_b L} & -1 \\ -\sin \hat{k}_b l & -\cos \hat{k}_b l & 1 & e^{-\hat{k}_b L} \\ -\cos \hat{k}_b l & \sin \hat{k}_b l & 1 & -e^{-\hat{k}_b L} \end{bmatrix} \begin{bmatrix} \hat{A}_1 \\ \hat{A}_2 \\ \hat{A}_3 \\ \hat{A}_4 \end{bmatrix} = \begin{bmatrix} 0 \\ 0 \\ 0 \\ \dfrac{F}{\hat{k}_b^3 \hat{D}} \end{bmatrix}. \tag{6}$$

The above matrix system of equations is solved to obtain the unknown coefficients $\hat{A}_1 - \hat{A}_4$, and consequently, the beam displacements, potential and kinetic energy. Due to the standing wave, the magnitude

of the potential energy stored in the system shows a cyclic variation with frequency. The potential energy becomes maximum at the resonance frequencies. The amount of the decreased potential energy is most significant when damage occurred at locations where the radius of curvature ($\partial^2 w/\partial x^2$) is largest. The sensitivity of the dynamic bending stiffness on damage depends on the relative amounts of the potential energy stored at the damage location to average potential energy stored in the structure and is calculated as

$$\mathrm{SD}(x,\omega) = \frac{D}{2(V/L)}\left(\frac{\partial^2 w(x,\omega)}{\partial x^2}\right)^2. \tag{7}$$

If damage occurred at x and sensitivity, SD, is large, there is a significant reduction in the dynamic bending stiffness obtained at frequency ω. Fig. 3 shows the dependence of sensitivity on the frequency and the damage location for the cantilever beam. The sensitivity was largest when the damage location was close to the fixed end of the beam ($x = 0$). It was relatively small when damage was located at the free end. In between the two extremes, the sensitivity exhibited cyclic variation with frequency and location. The variation of the sensitivity with frequency was not identical when the damage location was different. The number of local maximum increased with the increasing frequency. Its variation also depends on the boundary conditions. Fig. 4 shows the variation for the free–free beam excited at the free end. The four boundary conditions are

$$\frac{\partial^2 \hat{w}(0)}{\partial^2 x} = 0, \quad \frac{\partial^3 \hat{w}(0)}{\partial^3 x} = 0, \quad \frac{\partial^2 \hat{w}(L)}{\partial^2 x} = 0, \quad \hat{D}\frac{\partial^3 \hat{w}(L)}{\partial^3 x} = F. \tag{8a–d}$$

Using the same procedure as for the cantilever beam, the sensitivity was calculated. The sensitivity was small when damage occurred at free ends of the beam. Similarly to the cantilever beam, the sensitivity showed cyclic variation with frequency. Its variation depended on the damage location. Wide variety of boundary conditions such as spring supported ends should be constructed based on the actual supporting mechanism of structures. The sensitivity can be calculated following the same procedures.

From the variation of the measured dynamic properties and comparison to sensitivity of the dynamic bending stiffness, the damage location was identified. From the measured values and by monitoring the change of the dynamic bending stiffness, $\Delta D(\omega_k) = D_{\text{undamaged}} - D_{\text{damaged}}$, the damage indicator (DI) was calculated as

$$\mathrm{DI}(x) = \left|\sum_{k=1}^{n} \Delta D(\omega_k)\mathrm{SD}(x,\omega_k)\right| \tag{9}$$

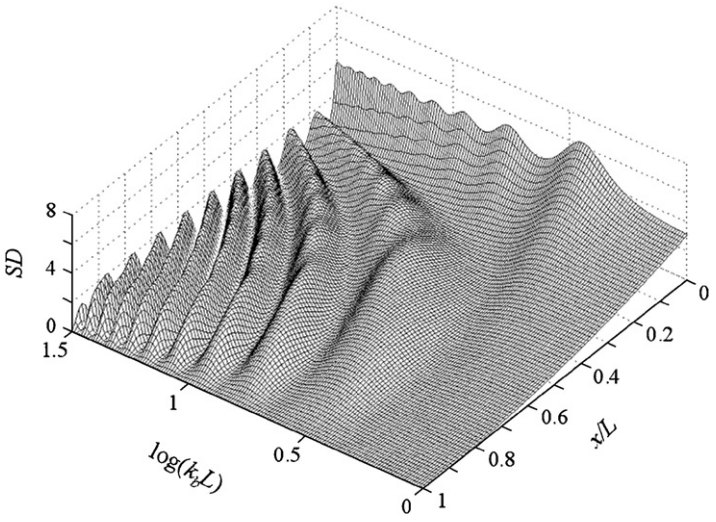

Fig. 3. Sensitivity variation with the frequency and damage location for cantilever beams.

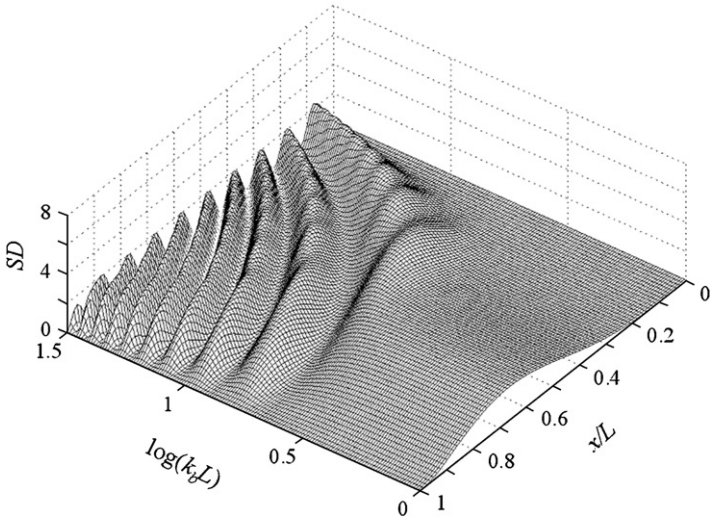

Fig. 4. Sensitivity variation with the frequency and damage location for beams with free–free boundary conditions.

This damage indicator was calculated from $x = 0$ to L. Among the calculated values, the location resulting in the maximum values was identified. The maximum and large absolute value of DI compared to values obtained for undamaged structures suggests that damage has occurred at that location.

The loss stiffness ($= \eta_D D$) was not used in obtaining the damage indicator since the reduction in the loss stiffness due to damage was not expected. For calculation of the damage indicator, the change in the dynamic bending stiffness is required. This change is measured and monitored using the beam transfer function method.

2.3. Beam transfer function method

The beam transfer function method is the experimental method of measuring the flexural stiffness of arbitrary beam structure [16]. To obtain the wave propagation characteristics from the measured vibration responses, the predicted beam displacement is compared to the measured value as

$$\Lambda e^{i\phi} = \frac{\hat{w}(x_1)}{\hat{w}(L)} = \frac{\hat{A}_1 \sin \hat{k}_b x_1 + \hat{A}_2 \cos \hat{k}_b x_1 + \hat{A}_3 e^{\hat{k}_b(x_1 - L)} + \hat{A}_4 e^{-\hat{k}_b x_1}}{\hat{A}_1 \sin \hat{k}_b L + \hat{A}_2 \cos \hat{k}_b L + \hat{A}_3 + \hat{A}_4 e^{-\hat{k}_b L}}, \tag{10}$$

where Λ is the amplitude and ϕ is the phase of the measured transfer functions between the displacements. Then, the Newton–Rapson method was applied to solve Eq. (10) with respect to the complex wavenumber, $\hat{k}_b = k_{br} - ik_{bi}$. After separating the real and imaginary parts, the iterations to solve the above equation are conducted as

$$\begin{bmatrix} k_{br} \\ k_{bi} \end{bmatrix}_{j+1} = \begin{bmatrix} k_{br} \\ k_{bi} \end{bmatrix}_{j} - \begin{bmatrix} \mathrm{Re}\left\{ \dfrac{\partial \hat{w}(x_1)}{\partial k_{br}}, \dfrac{\partial \hat{w}(x_1)}{\partial k_{bi}} \right\} \\ \mathrm{Im}\left\{ \dfrac{\partial \hat{w}(x_1)}{\partial k_{br}}, \dfrac{\partial \hat{w}(x_1)}{\partial k_{bi}} \right\} \end{bmatrix}^{-1} \begin{bmatrix} \mathrm{Re}\{\hat{w}(x_1) - \hat{w}(L)\Lambda e^{i\phi}\} \\ \mathrm{Im}\{\hat{w}(x_1) - \hat{w}(L)\Lambda e^{i\phi}\} \end{bmatrix}, \tag{11}$$

where the subscripts j and $j+1$ denote the current and next iterations, respectively. Using the complex wavenumber obtained through the Newton–Rapson method, the complex bending stiffness was consequently obtained

$$\hat{D} = \frac{\omega^2 M}{\hat{k}_b^4}. \tag{12}$$

The measured dynamic bending stiffness is the real part of the complex stiffness in Eq. (12) and used in the damage identification.

3. Results and discussion

To verify the proposed monitoring methods, experiments were performed using Plexiglas beams. The length, width and thickness of the beams were 0.77, 0.02 and 0.02 m, respectively. One end of the beam was fixed. The other end of the beam was excited by an impact hammer. The resulting vibration of the beam was measured using miniature piezoelectric accelerometers (Endevco model 2250-A) located at $x_1 = 0.62$ m and free end ($x = L$). Care was taken to prevent double impacts and to generate a force as consistent as possible.

Fig. 5 shows the measured transfer function between the beam displacements when damage (crack) was generated at $x = L/2$ and $2L/3$ by saw-cut. The measured transfer functions were very similar to the predicted values using Eq. (10) when there is no crack. As the crack depth, h_c, was increased, the measured resonance frequencies decreased. Depending on the damage location, there is a significant difference in frequency-dependent variation of the measured transfer function. If this information is used in structural health monitoring, it may result in a better identification compared to prediction by natural frequency alone. However, the information about damage cannot be obtained directly from this variation since it is influenced also by the modal responses. In addition, there was no significant change in the measured transfer function until the crack depth reached 6 mm (30% loss in the beam cross-sectional area).

Instead of using the measured transfer function directly for structural health monitoring, the dynamic properties were obtained. Fig. 6 shows the measured properties for undamaged beam. The bending stiffness became larger with the increasing frequency. The loss factor was less than 0.1 and continued to decrease with the increasing frequency. This value and its frequency-dependent variation were similar to those reported in Ref. [16].

When damage was induced, the obtained bending stiffness did not increase monotonically but showed cyclic variation with frequency as shown in Fig. 7. For the beams tested, the variation of the sensitivity of the dynamic bending stiffness with frequency was calculated using Eq. (7), as shown in Fig. 8. With the increasing crack depth, the measured dynamic bending stiffness varied as predicted by the sensitivity of the dynamic bending stiffness in Fig. 8. One method to find the damage location is a visual comparison of the change in the dynamic bending stiffness shown in Fig. 7 with the predicted sensitivity in Fig. 8, which provides an

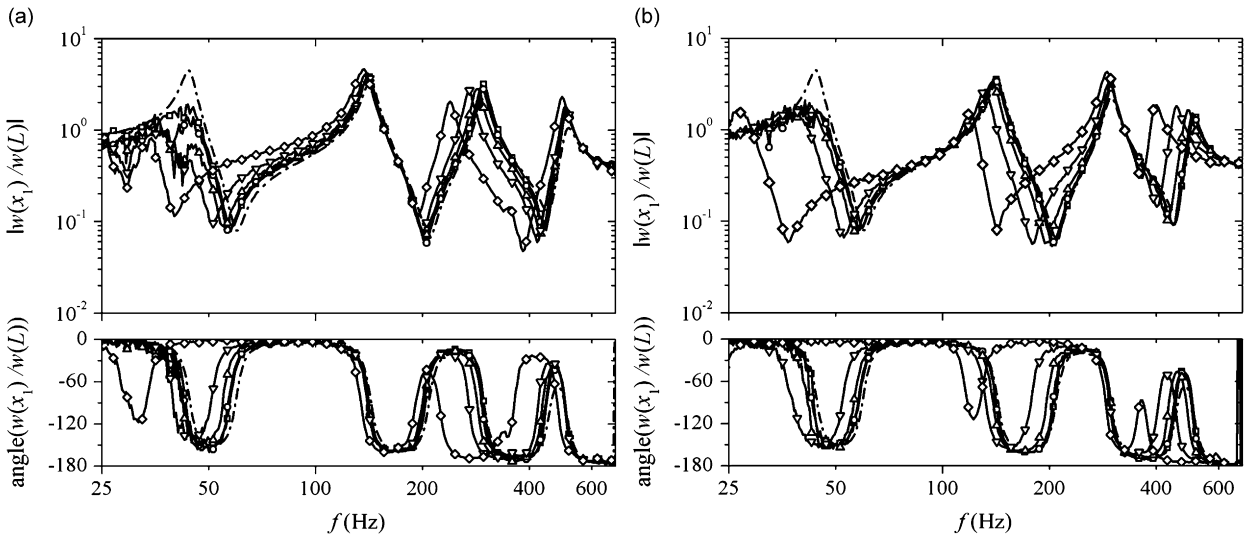

Fig. 5. Measured transfer function for different locations and magnitudes of damage, h_c/t: —□—, 0; —○—, 0.2; —△—, 0.4; —▽—, 0.6; —◇—, 0.8, and predictions for homogeneous beam (–· –· –·). (a) $x_c = L/2$ and (b) $x_c = 2L/3$.

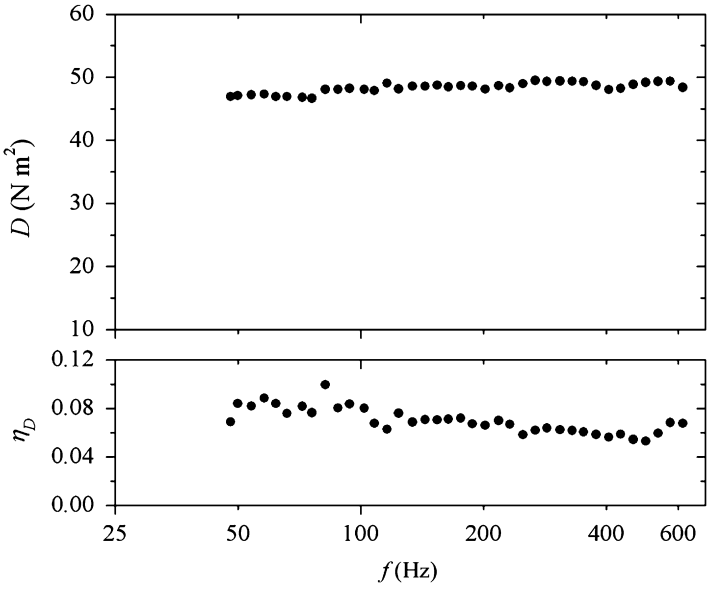

Fig. 6. Measured complex bending stiffness of the undamaged beam.

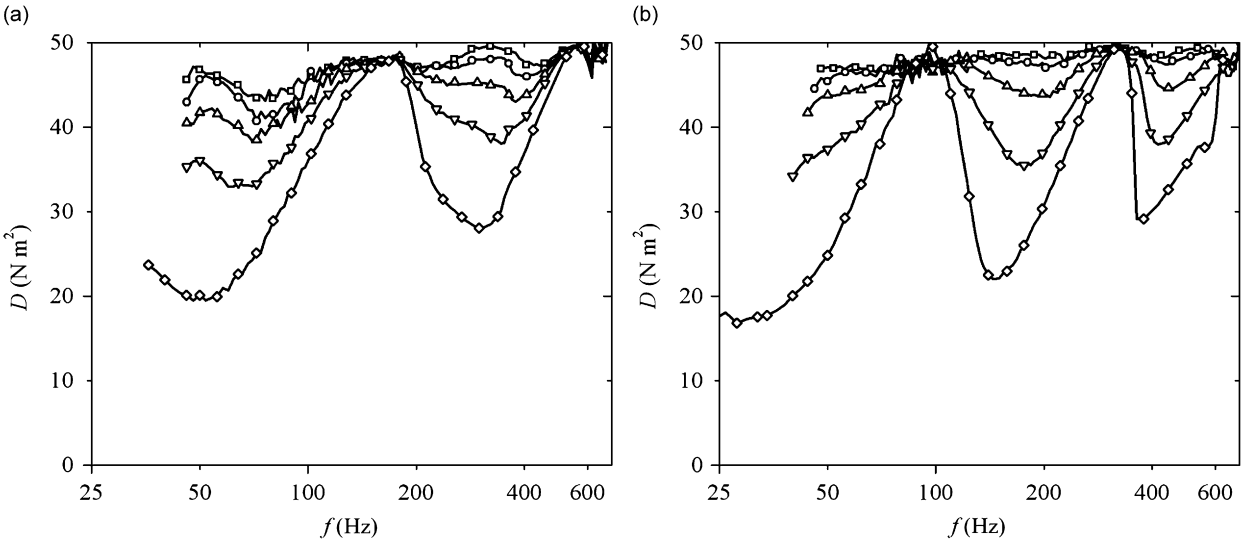

Fig. 7. Variation of the measured dynamic bending stiffness for different locations and magnitudes of damage, h_c/t: —□—, 0; —○—, 0.2; —△—, 0.4; —▽—, 0.6; —◇—, 0.8. (a) $x_c = L/2$ and (b) $x_c = 2L/3$.

approximate location. To determine the exact location, the DI was obtained as shown in Fig. 9. The sensitivity in Fig. 3 was used in the calculation. Theoretically the indicator function should be zero when undamaged. Due to several experimental uncertainties in measuring the transfer function, it does not converge to zero. However the magnitude should be small. With increasing crack depth there was significant increase in the damage indicator, DI.

There are several local maxima in the calculated damage indicator. Among the local maxima, the first or second maximum values were picked out. The crack location resulting in this maximum was identified (Fig. 9) and is tabulated in Table 1. The locations were identified within errors less than 1–4% when the crack magnitude is larger than 2 mm ($h_c/t = 0.1$). In Table 2, the beams with the crack induced at nine different

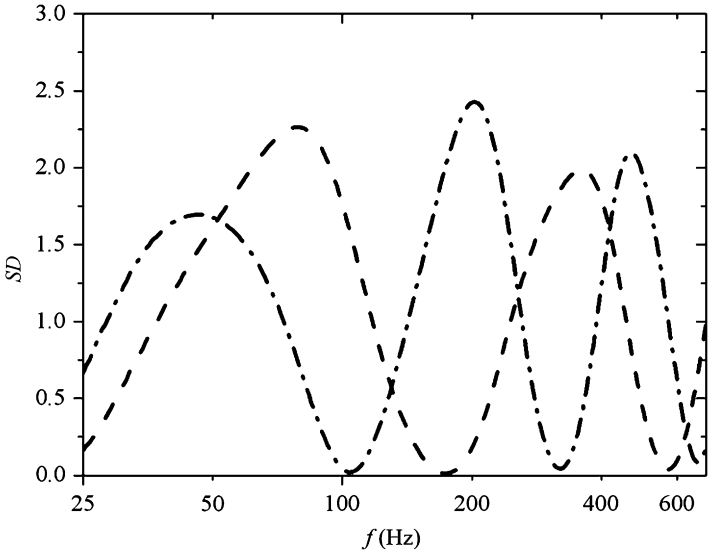

Fig. 8. Sensitivity variation with damage location, x_c: – – – – –, $L/2$; –· –· –·, $2L/3$.

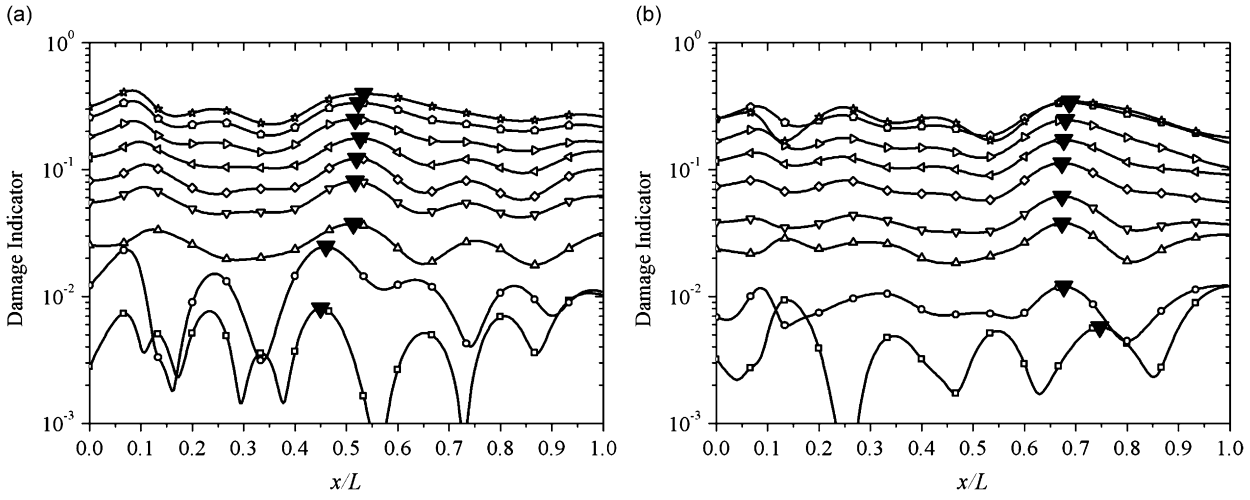

Fig. 9. Damage indicator and identified locations (▼) of damage for different crack depth, h_c/t: —□—, 0.1; —○—, 0.2; —△—, 0.3; —▽—, 0.4; —◇—, 0.5; —▷—, 0.6; —◁—, 0.7; —⬠—, 0.8; —☆—, 0.9. (a) $x_c = L/2$ and (b) $x_c = 2L/3$.

locations were also tested, and the estimated locations were tabulated. The proposed method resulted in accurate localization of damage for the different crack magnitudes and locations. Even when there was no significant variation in the measured transfer function, for example, $h_c/t < 0.2$, in Fig. 5, the location was identified accurately.

In the proposed health monitoring method, only two vibration measurements are necessary. It was not obvious whether the first or the second maximum value of the damage indicator resulted in the actual damage location. If the sensitivity calculated using Eq. (7) and the reduction in the dynamic bending stiffness is orthogonal, there should be only one maximum. However, there is no orthogonality condition in between the sensitivity and the reduction of the dynamic bending stiffness since the sensitivity was calculated as a positive real number. Also, the reduction is affected by the mechanical properties of the crack. A large number results when the location of damage is assumed to be located where the potential energy is large. This location

Table 1
Comparison of damage location estimated from first or second maximum of damage indicator to true value for various crack magnitudes (percentage of error in parenthesis)

Crack depth (h_c, mm)	True value, $x_c/L = 0.5$		True value, $x_c/L = 0.667$	
	Estimated value, x_c/L		Estimated value, x_c/L	
	First maximum	Second maximum	First maximum	Second maximum
2	–	0.45 (5%)	–	0.747 (8%)
4	0.46 (4%)	–	–	0.677 (1%)
6	0.513 (1.3%)	–	0.673 (0.7%)	–
8	0.517 (1.6%)	–	0.673 (0.7%)	–
10	0.52 (2%)	–	0.673 (0.7%)	–
12	0.527 (2.7%)	–	0.677 (1%)	–
14	0.517 (1.7%)	–	0.68 (1.3%)	–
16	–	0.523 (2.3%)	0.687 (2%)	–
18	–	0.533 (3.3%)	0.69 (2.33%)	–

Table 2
Comparison of damage location estimated from first or second maximum of damage indicator to true value when crack ($h_c = 4$ mm) was induced at various locations (percentage of error in parenthesis)

True value, x_c/L	Estimated value, x_c/L	
	First maximum	Second maximum
0.11	0.13 (1.9%)	–
0.22	0.23 (0.778%)	–
0.33	–	0.32 (1.3%)
0.44	0.447 (0.2%)	–
0.5	0.46 (4%)	–
0.56	0.557 (0.1%)	–
0.67	–	0.677 (1%)
0.78	–	0.737 (4%)
0.89	–	0.891 (0.1%)

experiences large strain when the structure vibrates and should be inspected when damage in the structure is anticipated. Based on one or two values that induce maximum of the damage indicator, the location and magnitude of crack was identified.

The absolute value of the damage indicator is not directly related to the actual magnitude of the crack. However, this information can be obtained from experiments using actual systems or from numerical model predictions beforehand, and used for estimating actual crack magnitude during real-time health monitoring of structures.

4. Conclusions

The method to identify damage in a beam structure using the flexural wave propagation was presented. The beam vibration characteristics were measured using the beam transfer function method. The frequency-dependent variation in the dynamic properties due to damage was predicted from the wave propagation approach and the system potential energy. Using this sensitivity and the variation of the equivalent dynamic bending stiffness, the location was monitored accurately using a small (two) number of vibration measurements even when the magnitude of damage is small. Since the temperature or surrounding fluid loading effects do not yield cyclic variation in the measured dynamic bending stiffness, their effects can be distinguished from those of damage. The proposed method utilizes the frequency-dependent variation of the

dynamic properties and the system potential energy. Consequently, the method is applicable even when damage occurred at nodes of the standing waves. Since the identification process does not require complicated numerical model or adaptive iterations, it does not require long computational time, which is advantageous for continuous real-time structural health monitoring.

Acknowledgment

This work was supported by the Korea Research Foundation Grant funded by the Korean Government (MOEHRD, Basic Research Promotion Fund) (KRF-2006-331-D00014).

References

[1] S.W. Doebling, C.R. Farrar, M.B. Prime, A summary review of vibration based damage identification method, *Shock and Vibration Digest* 30 (1998) 91–105.
[2] J.K. Sinha, M.I. Friswell, S. Edwards, Simplified models for the location of cracks in beam structures using measured vibration data, *Journal of Sound and Vibration* 251 (2002) 13–38.
[3] D.P. Patil, S.K. Maiti, Experimental verification of a method of detection of multiple cracks in beams based on frequency measurements, *Journal of Sound and Vibration* 281 (2005) 439–451.
[4] S.S. Law, Z.R. Lu, Crack identification in beam from dynamic responses, *Journal of Sound and Vibration* 285 (2005) 967–987.
[5] C.R. Farrar, D.A. Jauregui, Comparative study of damage identification algorithms applied to a bridge: I. Experiment, *Smart Materials and Structures* 7 (1998) 704–719.
[6] C.P. Ratcliffe, Damage detection using a modified Laplacian operator on mode shape data, *Journal of Sound and Vibration* 204 (1997) 505–517.
[7] A.S.J. Swamidas, Y. Chen, Monitoring crack growth through change of modal parameters, *Journal of Sound and Vibration* 186 (1995) 325–343.
[8] D.E. Adams, M. Nataraju, A nonlinear dynamical systems framework for structural diagnosis and prognosis, *International Journal of Engineering Science* 40 (2002) 1919–1941.
[9] L.J. Hadjileontiadis, E. Douka, A. Trochidis, Crack detection in beams using kurtosis, *Computers and Structures* 83 (2005) 909–919.
[10] J. Ma, D.J. Pines, Dereverberation and its application to damage detection in one-dimensional structures, *AIAA Journal* 39 (2001) 902–918.
[11] S.S. Kessler, S.M. Spearing, C. Soutis, Damage detection in composite materials using Lamb wave methods, *Smart Materials and Structures* 11 (2002) 269–278.
[12] L. Mallet, B.C. Lee, W.J. Staszewski, F. Scarpa, Structural health monitoring using scanning laser vibrometry: II. Lamb waves for damage detection,, *Smart Materials and Structures* 13 (2004) 261–269.
[13] M. Lemistre, D. Balageas, Structural health monitoring system based on diffracted Lamb wave analysis by multiresolution processing, *Smart Materials and Structures* 10 (2001) 504–511.
[14] J.W. Ayres, F. Lalande, Z. Chaudhry, C.A. Rogers, Qualitative impedance-based health monitoring of civil infrastructures, *Smart Materials and Structures* 7 (2001) 599–605.
[15] G. Park, H.H. Cudney, D.J. Inman, An integrated health monitoring technique using structural impedance sensors, *Journal of Intelligent Material Systems and Structures* 11 (2001) 448–455.
[16] J. Park, Transfer function methods to measure dynamic mechanical properties of complex structures, *Journal of Sound and Vibration* 288 (2005) 57–79.